



## Research Article

## Performance Evaluation of Regression-Based MPPT Algorithms Using Inverse SEPIC Converter under Partial Shading

Zaiba Ishrat<sup>a</sup>, Preeti Singhwal<sup>b</sup>, Taslima Ahmed<sup>c</sup>, Yogendra Chhetri<sup>d</sup>, Arpana Mishra<sup>e</sup>, Kunwar Babar Alif<sup>f</sup>

<sup>a</sup>Department of ECE, Meerut Institute of Technology, Meerut, UP, India.

<sup>b</sup>Faculty of Managemt & Commerce, Swami Vivekanand Subharti University, Meerut, UP, India.

<sup>c</sup>Department of ECE, IIMT College of Engineering, Greater Noida, UP, India.

<sup>d</sup>Departmnet of Centre for Continuing Education, Indian Institute Of Science, Bengaluru, Karnataka, India.

<sup>e</sup>Department of CS&IT, Dronacharya Group Of Institutions, Greater Noida, India.

<sup>f</sup>Department of CSE(AI/ML), Meerut Institute of Engineering & Technology, Meerut, UP, India.

## PAPER INFO

## Paper history:

Received: 04 March 2025

Revised: 05 November 2025

Accepted: 05 December 2025

## Keywords:

Linear Regression Based Technique,  
Maximum Power Point Tracking,  
Partial Shading Condition,  
Solar Photovoltaic System MATLAB/Simulink

## A B S T R A C T

Numerous green energy resources, including solar, wind, bio, and hydropower, have garnered significant attention as effective alternative energy sources. Particularly beneficial to society and the economy, solar photovoltaic systems (SPVS) are the most preferred resource. Unfortunately, because of shadowing situations and fluctuating loads, these systems are unable to maximize power extraction under changeable irradiance. Many Lower Peak Power Points (LPPPs) and Global Peak Power Points (GPPPs) on their power voltage characteristics (P-VC) arise as a result of PSC. Therefore, these systems employ Maximum Power Point Tracking (MPPT) approaches. This work implements and experimentally evaluates two supervised learning MPPT schemes, Support Vector Regression (SVRT) and Linear Regression Based Technique (LRBT), for stand-alone photovoltaic systems under partial shading, using an inverse SEPIC converter. The main novelty is a hardware-aware, real-time evaluation of a computationally light LRBT MPPT on an inverse SEPIC topology, and a comparative analysis against SVRT on metrics relevant to practical deployment, including computational complexity, tracking time, output power or current, and tracking efficiency, under realistic partial shading conditions. Unlike prior ML studies that rely on simulation or heavy models, LRBT demonstrates fast convergence and very low computational cost suitable for microcontroller implementation. In MATLAB/Simulink experiments on a 2×2 PV array and inverse SEPIC converter, LRBT achieves a mean tracking efficiency of 98.3% (±0.25%), reduces tracking time to approximately 0.10 s (variance 0.0008 s), and improves delivered power by about 2.0–3.0% relative to SVRT under the tested shading patterns. LRBT's model size and prediction speed make it significantly more suitable for low-cost real-time hardware compared to SVRT.

<https://doi.org/10.30501/jree.2025.506604.2273>

## 1. INTRODUCTION

Researchers are compelled to explore alternative energy sources as the world's energy consumption grows, the accessibility of fossil fuels diminishes, and pollution levels rise. Solar power generation with SPVS is the most encouraging renewable energy source, which does not require any rotating parts and is environmentally friendly. It simply requires freely available sunlight. One of the main drawbacks of these systems is their strong reliance on solar irradiation, which causes a variable power yield at the output. When the SPVS receives uniform irradiance, its P-VC has a single peak known as GPPP. As illustrated in Fig. 1, several MxPP occur on the P-VC when PSC cause the SPVS to receive uneven illumination. The lesser peak values in a P-VC are referred to as LPPP, while the uppermost power peak is referred to as GPPP, except the highest peak. In order to attain the true GPPP during PSC, MPPT systems are sometimes combined

with SPVS. One of the issues that concern MPPT designers is an algorithm's capacity to pursue GPPP during a shading instance. One of the primary reasons for multiple power peaks (LPPP and GPPP) with irregular trajectories is partial shading. The P-VCs are shaped in such a way that the MPPT can no longer track the real GPPP.

\*Corresponding Author's Email: [zaibaishrat01@gmail.com](mailto:zaibaishrat01@gmail.com) (Z. Ishrat)

URL: [https://www.jree.ir/article\\_238093.html](https://www.jree.ir/article_238093.html)

Please cite this article as: Ishrat, Z., Singhwal, P., Ahmed, T., Chhetri, Y., Mishra, A., & Babar Ali, K. (2026). Performance Evaluation of Regression-Based MPPT Algorithms Using Inverse SEPIC Converter under Partial Shading, *Journal of Renewable Energy and Environment (JREE)*, 13(2), 12-21. <https://doi.org/10.30501/jree.2025.506604.2273>.



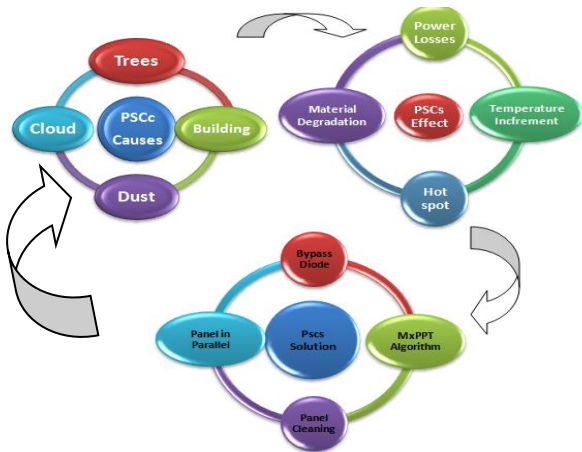


**Figure 1.** PSC Root causes effect and solution

General MPPT approaches, such as Hill climbing [Rawat et al. 2013], PnO [Piegari et al. 2017], HCg [Piegari et al. 2017], and INCA [Podder et al. 2019], are proven more efficient in calculating real MXmPP for homogeneous irradiance with a noticeable peak on P-VCs. Nevertheless, these methods often belong to one of the LPPPs under PSC and fail to guarantee world-wide convergence, leading to power loss [Podder et al. 2017; Ishrat et al. 2023; Mosa et al. 2017]. Later on, these methods have been modified to track GPPP under PSC [Podder et al. 2019, Ishrat et al. 2023, Mosa et al. 2017, Kamarzaman et al. 2014, Mustafa et al. 2020]. Researchers have focused on various artificial intelligence-based MPPT strategies to address complex problems that resulted from PSC [Mosa et al. 2017, Karami et al. 2017, Liu et al. 2014, Mohapatra et al. 2017]. The GPPP can be determined using a metaheuristic algorithm, with MxPPTMPPT identified as an optimization problem. Based on the population approach, a number of swarm intelligence [Nugraha et al. 2017, Hayder et al. 2020, Ahmed et al. 2014] and bio-inspired [Abu et al. 2020, Belghith et al. 2016, Rezk et al. 2017] methods were examined. Moreover, the aforementioned modifications made to improve their performance were reported [Pilakkat et al. 2020, Martínez et al. 2021]. ANN [Tey et al. 2018], evolutionary algorithms [G. Tandel et al. 2016], and FLC [Takun et al. 2011, Tey et al. 2018] were also utilized in PSC to monitor GPPP. In the past few years, numerous hybrid approaches have also been reported, combining two or more MPPT procedures to leverage their respective features [Batarseh et al. 2018, Priyadarshi et al. 2019, Manickam et al. 2016]. By combining the traditional method with the bio-inspired (INC-DFO) approach, the authors [Sarwar et al. 2022] demonstrated a novel idea for GPPP tracking under PSC with an average efficiency of 99.92%. Another study [Sharmin et al. 2022], the Bayesian network-based method is suggested for maximizing the total power yield of the PV arrangement while minimizing steady-state fluctuations and monitoring time. The proposed strategy is 99% accurate at following the GPPP within 2 s and responds to load variations within 0.1 s. A SEPIC converter is used in [Memaya et al. 2019] and simulated on MATLAB. A localized version of the SVM and ELM supervised MLA [Du et al. 2018] eliminates the necessity for regular parameter training. Takuri et al. [Takuri et al. 2020] also employed SVM to predict the optimal reference voltage of a photovoltaic setup in the presence of changing load conditions, temperature, and solar irradiance. Ishrat et al.

compared two regression-based techniques for MPPT of SPVS [Ishrat et al. 2023]. A comparative analysis of ML-based MPPT techniques was proposed by different scholars in [Ishrat et al. 2024a; Ishrat et al. 2024b; Nkambule et al. 2020; Sun et al. 2019]. The authors [Al et al. 2024] provides a comprehensive review of advanced metaheuristic and hybrid MPPT algorithms for solar photovoltaic power generation, identifying Grey Wolf Optimization and Jaya-Differential Evolution as leading techniques for maximizing power extraction under variable conditions. Its major finding is that these algorithms outperform conventional methods, especially when validated experimentally on industrial-scale PV systems. However, the study is limited by a lack of uniform test conditions, which makes direct performance comparison and practical recommendations challenging. In terms of computational complexity, hardware implementation feasibility, and computational time, each of these intelligent strategies varies from the others. Table 1 provides an examination of newly published intelligent techniques based on significant MPPT features.

The following are the main goals of the current study:

- Software deployment of standalone SPVS using inverse SEPIC and resistive load along with LRBT and SVRT MPPT techniques.
- Performance appraisal in real time of two MPPT techniques (SVRT and LRBT) under varying environmental conditions.
- Comparative evaluation of SVRT and LRBT on several metrics when monitoring GPPP in test scenarios.

**Novelty of work:** Imagine a home solar energy system installed on a rooftop in an area with fluctuating weather patterns, including intermittent shade from adjacent trees and structures during the day. Conventional MPPT controllers frequently face difficulties in optimizing power extraction during dynamic shading because of various local maxima in the power voltage curve created by shading. In such a case, the suggested LRBT MPPT controller employs regression machine learning to quickly and precisely determine the global maximum power point in real time. For example, when the shadows of a moving cloud diminish sunlight intensity on a section of the array, the controller promptly modifies the duty cycle of the SEPIC converter to follow the new optimal operating point within a short duration. This rapid reaction reduces power loss, resulting in an average power efficiency exceeding 98% even under varying conditions.

This work's novelty can be summed up as a set-theoretic presentation and comprehensive performance evaluation emphasizing technical datasheet-style reporting of the primary characteristics of two distinct MPPT techniques. The novel points of this research are as follows:

- a) Lightweight LRBT suitable for microcontroller implementation due to the simplicity of the model.
- b) First real-time evaluation on inverse SEPIC topology in this configuration under varying environmental conditions.
- c) Quantitative comparison of SVRT and LRBT that highlights LRBT's favorable trade-offs in tracking time, computational complexity, and output power in real-time-like tests.

**Table 1** Review of the latest work to track GPPP under PSC.

Author(Reference)	AI-MPPT	Hardware Used	Converter	Software used	Error	Tracking Duration	Maximum efficiency
<a href="#">Keyrouz et al. 2018</a>	BNN-MPPT	Arduino & DSP	Boost	Matlab	Mean absolute error=4%	1.76s	97.89%
<a href="#">Memaya et al. 2019</a>	DE-MPPT	PVUE125MF5N	SEPIC	PowerSim	Error Margin=1%	2s	99%
<a href="#">Du. et al 2019</a>	SVM&ELM	R-305E-WHT-D	Boost	Matlab	Mean Absolute error=0.083	.02sec-.15sec	94.52%
<a href="#">Radjai et al. 2014</a>	MLVR-P&O	dSPACE DS1104	Buck	Python	Error Margin=0.5%	.08sec-.2sec	99.8%
<a href="#">Sharmin et al. 2022</a>	BNN-P&O	ZM-A-M-100	Boost	Matlab	MSE= 2.87*10 <sup>-3</sup>	Not Specified	99.594%
<a href="#">Kalogerakis et al. 2020</a>	Q Learning	DSP	Boost	Matlab	MSE=0.1-1%	.04sec-0.2 sec	99.3-99.6%
<a href="#">Mahesh et al. 2022</a>	DTR	Arduino & DSP	Boost	Matlab	Low RMSE	0.6s	93.99%
<a href="#">Farayola et al. 2018</a>	LIR	1STH-215-P module	Cuk	Psim	RMSE=5.5339e-7	.05sec-.2sec	73.24%

LRBT outperforms other intelligent approaches documented in the literature in terms of T, E, CC, OP, and OC, according to test validation and relative analysis conducted in real-time surroundings. The remaining sections of this manuscript are organized as follows: The problem formulation is illustrated in Section 2, and the two MPPT AI approaches selected to analyze their GPPP performance under PSC are presented in Section 3. Section 4 provides the complete experimental setup. Section 5 discusses the effectiveness and outcomes of the chosen MPPT techniques. Section 6 outlines the study’s challenges and expanded scope, while Section 7 offers the conclusion.

**2. Modeling of SPVS**

An SPVS is made up of several solar panels consisting of solar cells connected in parallel and series. Since the single diode model (SDM) requires fewer parameters for accurate modeling and imposes less computational overhead, it is used to design and analyze SPVS. Figure 2 depicts the widely used SDM of an SPVS. The SPVS can be mathematically modeled under uniform irradiance using Functional Eq. (1), and its I-V relationship can be expressed as follows:

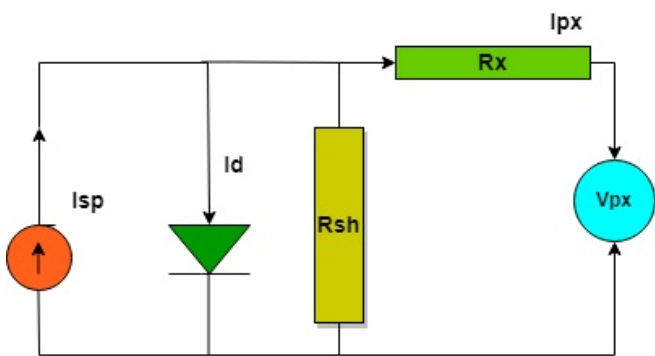


**Figure 2.** SDM of SPVS

$$I_p = I_{sp} - I_d - (V_{px} + I_{px}R_x)/R_p \tag{1}$$

$$I_{px} = N_p I_{sp} - N_y I_d - \frac{V_{px} + I_{px}R_{xnz}}{R_p * nz} \tag{2}$$

Where  $nz = N_y/N_p$

$$I_d = I_s \left( e^{\frac{q(V_{px} + I_{px}R_x)}{AKT N_y}} - 1 \right) \tag{3}$$

Figure 1 illustrates the various factors that contribute to deviations in incident radiation (PSC) on different modules within the SPVS, including reduced FF and power loss. Under

PSC, the harnessed power of several modules in the array will drastically drop, resulting in hotspots and unbalanced conditions throughout the system. This problem is mitigated by using bypass diodes. Moreover, temperature affects the SPVS's output, so different cooling strategies are employed to address this issue [[Bayrak et al. 2020](#), [Bayrak et al. 2019](#), [Sattar et al. 2022](#)]. By adding various materials, the structure can also achieve improved energy conversion [[Khan M. et al. 2022](#)].

This simulation is carried out on a 2x2 SPVS array, as displayed in Figure 3, using the SPVS module under the conditions mentioned in Table 2. To reduce the adverse effects that occur in SPVS due to PSC, this study evaluates MPPT techniques under three test conditions, as listed in Table 3, with SEPIC converters applied in each condition individually. Figure 3(a) shows the SPVS under PSC1, while Figures 3(b) and 3(c) show the SPVS under PSC2 and PSC3, respectively.

**Table 2.** Specifications of a user-defined unit solar cell model in Matlab/Simulink

Parameter	Value
OCV	7.5V
Isc	2.2A
Vmp	6V
Imp	1A
Pm	6W
Temperature Coefficient(Tc) of Voc (% /deg c)	-0.36099
Tc of Isc (% /deg c)	0.102
Ir	1.5A
Rsh	9.92ohm
Rx	0.035ohm

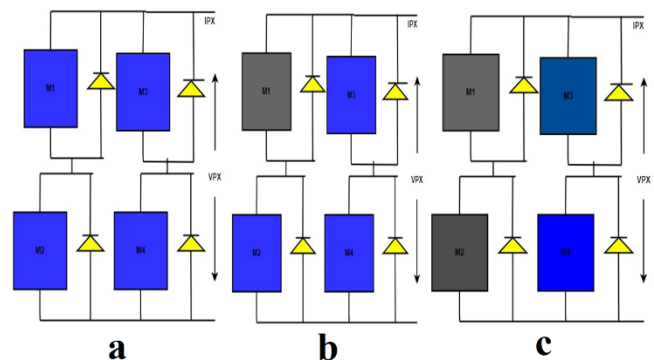


**Figure 3.** (a) PSC1, (b) PSC2 & (c) PSC3

**Table 3.** Operating Condition

Condition	Environment Condition
PSC1	(1000W/m <sup>2</sup> , & 25 °C)
PSC2	(800W/m <sup>2</sup> , & 25°C)
PSC2	(800W/m <sup>2</sup> , & 25°C)

### 3. AI MPPT Techniques

#### 3.1. Support Vector Machine Regression (SVRT)

Regression tasks, where the objective is to predict a continuous target variable instead of class labels, can also be implemented using SVRT. The main goal of SVR is to find a function, or a hyperplane in the feature space, that most accurately captures the relationship between the input parameters and the continuous target variable. The objective of SVR is to identify a hyperplane, also known as a regression line, that minimizes the difference between the predicted and actual target values while adhering to a predetermined margin. Minimizing the cost function, as provided by the equation, is the aim of SVRT ([Kumar Panda et al., 2023](#), [Beers 2024](#), [Alpaydin, n.d.](#), [Mohri et al., 2018](#), [Rasmussen, 2004](#), [Awan et al., 2021](#)).

$$J(w, B, \epsilon, \epsilon') = \frac{1}{2} \text{mod} \{w\}^2 + c \sum_{i=1}^n (\epsilon + \epsilon') \quad (5)$$

$W$  represents the weight and  $B$  represents the bias value,  $\epsilon$  and  $\epsilon'$  are the margin variables allowing for error, and  $C$  is the regularization parameter that controls the trade-off between error and the margin variables.

The regression function using SVRT is:

$$F(x) = W^T + B \quad (6)$$

where  $x$  is the input feature vector.

The new predicted values should lie within the margin, so limiting conditions are applied, as given in the equations:

$$Y_i - f(x_i) \leq \delta + \epsilon_i \quad (7)$$

$$f(x_i) - Y_i \leq \delta + \epsilon_i' \quad (8)$$

where  $Y_i$  is the target value for the  $i$ th data point,  $\delta$  is the acceptable error, and  $\epsilon_i, \epsilon_i'$  are slack variables.

A dual problem  $W(\beta, \beta')$  is created using Lagrange multipliers ( $\beta, \beta'$ ) for each constraint. The dual problem is to maximize the following equation:

$$W(\beta, \beta') = \sum_{i=1}^N (\beta_i - \beta_i') - \frac{1}{2} \left( \sum_{i=1}^N (\beta_i - \beta_i') \beta_j - \beta_j' \right) (x_i, x_j) \quad (9)$$

Subject to constraints:

$$0 \leq \beta, \beta_i' \leq C$$

$$\sum_{i=1}^N (\beta_i - \beta_i') = 0 \quad (10)$$

The weight vector,  $w$ , can be computed by

$$w = \sum_{i=1}^N (\beta_i - \beta_i') (x_{i1}, x_{i2}) \quad (11)$$

$$b = Y_s - \sum_{i=1}^N (\beta_i - \beta_i') (x_{i1}, x_{i2}) \quad (12)$$

To predict a new target value, the SVRT function is given as follows:

$$F(X_{\text{new}}) = w^T X_{\text{new}} + B \quad (13)$$

Table 4 presents the error estimation during the training and testing phases using the SVRT algorithm model.

**Table 4.** Error analysis of the SVRT Model

Error(Validation)			Error(Testing)		
RMSE	MSE	MAE	RMSE	MSE	MAE
0.0689	0.0047472	0.05806	0.06912	0.00472	0.0559
<b>Prediction</b>					<b>Speed</b>
1800obs/sec					
<b>Training</b>					<b>Time</b>
12.174sec					
<b>Model</b>					<b>Size</b>
4KB					

#### 3.2. Linear Regression Algorithm based technique (LRBT)

By applying a linear equation to empirical data, linear regression is a widely used supervised ML approach for modeling the relationship between a dependent variable (target) and one or more independent variables (features). It is a simple yet effective algorithm that is commonly applied in forecasting, prediction, and analyzing variable relationships. The linear regression model represents the relationship between the target variable ( $Y$ ) and the features ( $X$ ) as a linear equation ([Kumar Panda et al., 2023](#); [Beers, 2024](#); [Alpaydin, n.d.](#); [Mohri et al., 2018](#); [Rasmussen, 2004](#); [Awan et al., 2021](#)).

$$Y_x = \epsilon_0 + \epsilon_1 X_1 + \epsilon_2 X_2 + \dots + \epsilon_3 X_n + \epsilon \quad (14)$$

Where  $\epsilon_0$  is the intercept value and  $\epsilon_1, \epsilon_2$  are the coefficients that indicate the unit change in  $Y_x$  when there is a change in  $X$ , and  $\epsilon$  represents the acceptable error. The cost objective function for LRA is given in the following equation, which should be minimized:

$$\text{MSE} = \frac{1}{N} \sum_{i=1}^N (Y' - Y_x)^2 \quad (15)$$

where  $N$  is the number of data points,  $Y'$  is the predicted target value, and  $Y_x$  is the actual value. The main goal is to determine the coefficients that minimize the error. Table 5 presents the error estimation during the training and testing phases using the LRBT algorithm model.

**Table 5.** Error analysis of the LRBT Model

Error(Validation)			Error(Testing)		
RMSE	MSE	MAE	RMSE	MSE	MAE
0.01642	0.0047472	0.0143056	0.01644	0.0003135	0.014314
<b>Prediction</b>					<b>Speed</b>
4800obs/sec					
<b>Training</b>					<b>Time</b>
5.0871sec					
<b>Model</b>					<b>Size</b>
4KB					

#### 3.3. Proposed AI-MPPT Algorithm

Authors use the SVRT and LRBT methods to track the MXmPP of a SPVS. The steps of the proposed MPPT algorithm are listed below. Figure 4 illustrates the flow chart of the proposed MPPT algorithm.

- Evaluate the SPVS voltage  $V_{px}$  and current  $I_{px}$  for the given radiation and temperature conditions.
- Compute the instantaneous SPVS power  $P_x$ .
- Estimate the future maximum current  $I_{m\_pp}$  using the AI-MPPT model for the incident illumination and temperature.
- If the instantaneous current  $I_{px} < I_{m\_pp}$ , increase  $I_{px}$  by adjusting the duty cycle  $D_d$ .

- v. If the instantaneous current  $I_{px} > I_{m\_pp}$ , decrease  $I_{px}$  by adjusting the duty cycle  $D_d$ .
- vi. Repeat the procedure until  $I_{m\_pp} = I_{px}$ .
- vii. Compute  $P_x$  when the target is achieved and display the  $P_{max}$  of the SPVS.

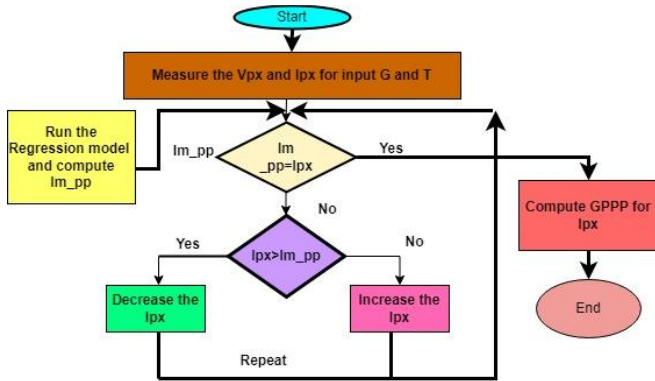


Figure 4. MPPT Algorithm Flow Chart

### 3.4. Simulation setup

A prototype experimental setup is used to test two AI approaches (Fig. 5). A standalone SPVS prototype is designed using four user-defined PV panels connected in a  $2 \times 2$  series-parallel configuration. An inverse SEPIC converter is employed to evaluate the performance of each technique. The method under consideration is tested for performance under PSC by integrating a resistive load into the SPVS. PSC are induced in the SPVS under non-uniform irradiance conditions using variable illumination. Figure 5 presents the block diagram of the MPPT arrangement.

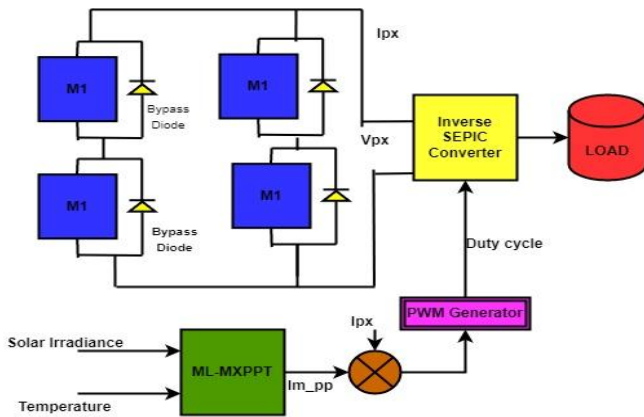


Figure 5. Block diagram of the MPPT

### 4. Inverse SEPIC DC converter

The SEPIC converter, also known as a zeta converter, is used to increase or decrease  $V_{in}$  to a regulated value using a simple and low-cost mechanism. The DC conversion ratio is given by Eq. (16) as follows:

$$V_{out}/V_{in} = D_n / (1 - D_n) \quad (16)$$

If  $D_n > 0.5$ , the SEPIC operates in boost mode; otherwise, it operates in buck mode. The inverse SEPIC converter design is discussed in [Putri et al., 2021, Moon et al., 2022, Gökkuş & Endiz, 2024], with its component specifications listed in Table 6.

Table 6. Specifications of the inverse SEPIC DC converter parameters

Parameter	Value
$V_{in-min}$	6V
Input Voltage Maximum	16 V
Output voltage Maximum	15V
Output current Minimum	1.2A
Output current Maximum	1.8 A
Output Power Minimum	18W
Output Power Maximum	24W
L1	0.165mh
L2	0.165mh
$R_o$	9.3ohm
C1&C2	88microfarad
f	100Khz
Change in inductor current	0.1
Change in capacitor voltage	0.4

### 5. Results and Discussion

Authors first evaluate the performance of MPPT approaches in tracking the GPPP under variable environmental conditions with a fixed load. The performance of each MPPT method (LRBT and SVRT) on a standalone SPVS with a  $2 \times 2$  SPV configuration, as shown in Fig. 5, is simulated in terms of output power, current, tracking time, and tracking efficiency. Each method is simulated in Matlab/Simulink under three varying solar illumination conditions, as summarized in Table 7. In PSC-1, all panels receive the same illumination intensity of  $1000 \text{ W/m}^2$ . In PSC-2, one SPV is shaded, receiving  $800 \text{ W/m}^2$ . In PSC-3, the SPVS is illuminated at  $600 \text{ W/m}^2$ . Figure 6 shows the voltage, current, and power under STC for the  $2 \times 2$  SPVS. Figure 7 shows the load output voltage, which remains almost constant across all shading patterns. Figures 8, 9, and 10 present the panel output current, SEPIC converter output current using LRBT, and SEPIC converter output current using SVRT under PSC-1. Figures 11, 12, and 13 show the corresponding currents under PSC-2. Figures 14, 15, and 16 depict the currents under PSC-3 for panel output current, LRBT converter output current, and SVRT converter output current, respectively.

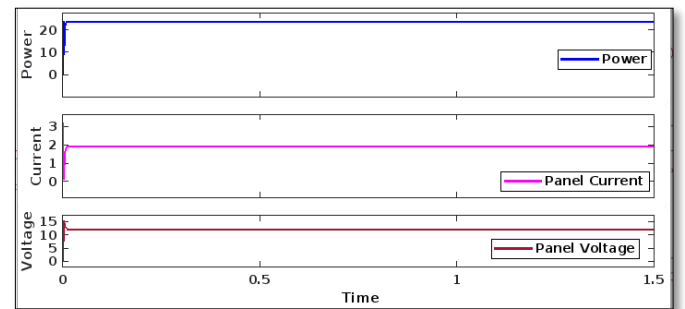
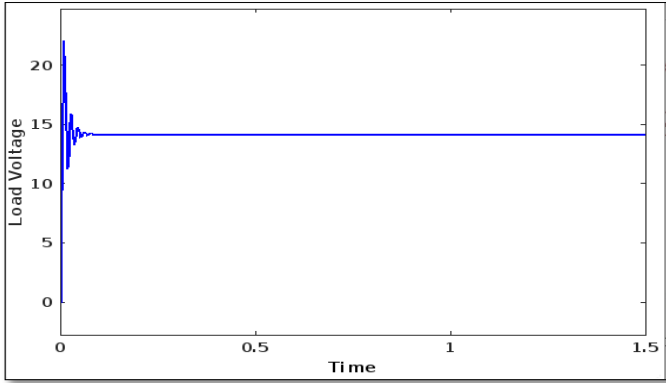


Figure 6.  $2 \times 2$  SPVS's voltage, current, and power under ( $1000 \text{ Watt/m}^2$ ,  $25^\circ\text{C}$ )

**Table 7.** Simulation Result of 2\*2 SPVS

Solar irradiance	Vin (v)	Iin (A)	Vout (v)	Iout (A)	$\eta$ (Pout/Pin)*100	Vin (v)	Iin (A)	Vout (v)	Iout (A)	$\eta$ (Pout/Pin)*100
	<b>LRBT</b>					<b>SVRT</b>				
PSC1(1000W/m <sup>2</sup> ,25 °C)	12	2.04	13.79	1.74	99.97	12	2	13.79	1.705	97.96
PSC2(800W/m <sup>2</sup> , 25°C)	12	1.805	13.79	1.553	98.87	12	1.805	13.79	1.513	96.32
PSC3(600W/m <sup>2</sup> , 25°C)	12	1.61	13.79	1.370	98.39	12	1.61	13.79	1.35	96.96



**Figure 7.** Load output voltage under (1000Watt/m<sup>2</sup>, 25°C)

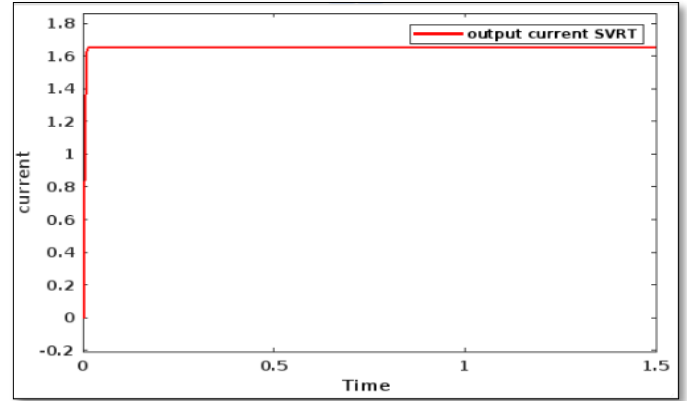


**Figure 10.** Load output current under (1000Watt/m<sup>2</sup>&25°C) using SVRT

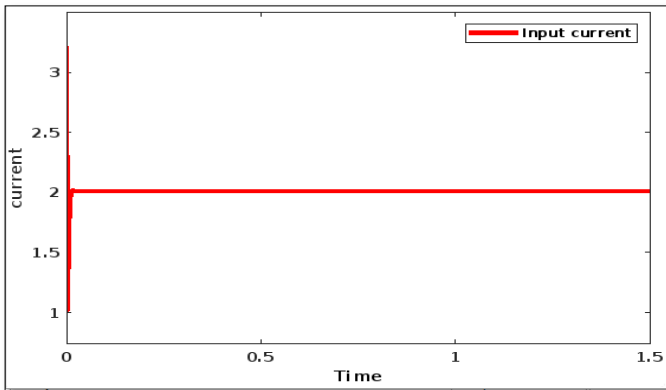


**Figure 8.** Panel output current under (1000W/m<sup>2</sup>, 25°C)

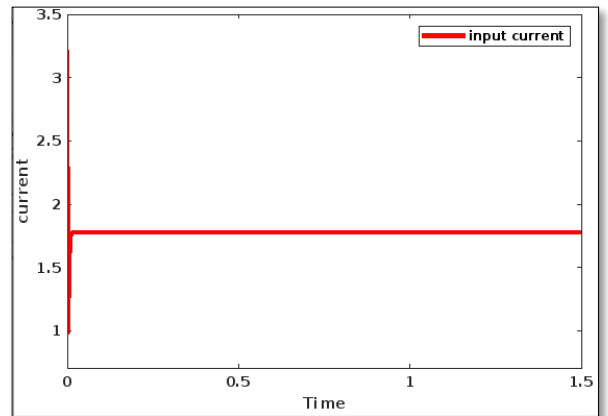


**Figure 11.** Panel output current under (800W/m<sup>2</sup>&25°C)

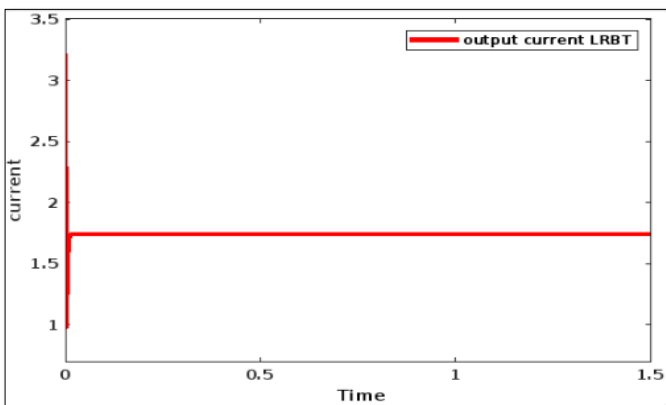


**Figure 9.** Load output current under (1000W/m<sup>2</sup>, 25°C) using LRBT

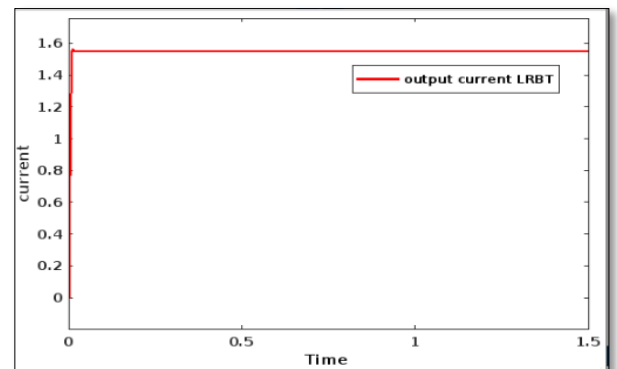


**Figure 12.** Load output current under PSC2(800Watt/m<sup>2</sup>, 25°C) using LRBT

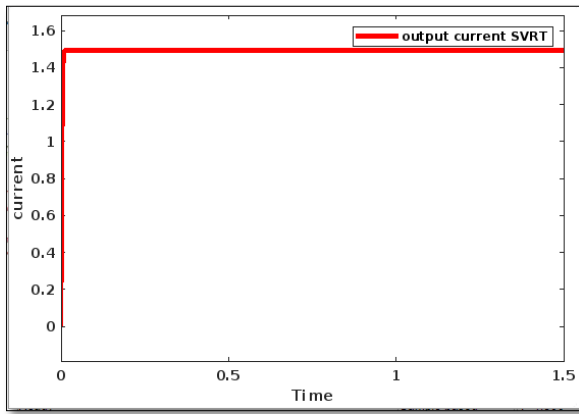


Figure 13. Load output current under PSC2 (800Watt/m<sup>2</sup>&25°C) using SVRT

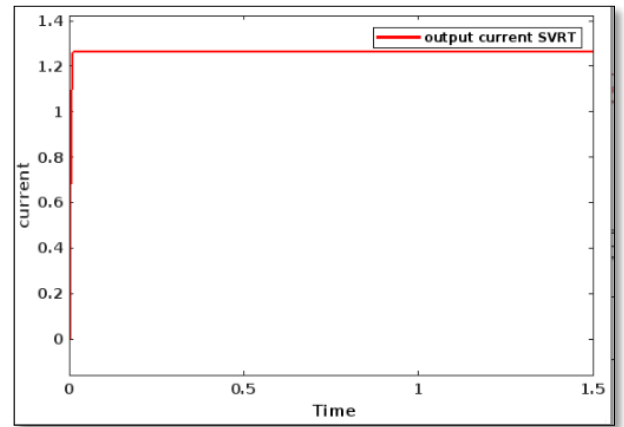


Figure 16. Load output current un PSC2(800Watt/m<sup>2</sup>, 25°C) with SVRT

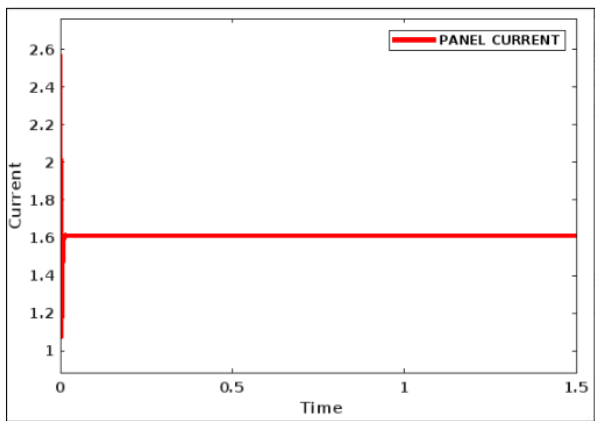


Figure 14. Panel output current under PSC2(600Watt/m<sup>2</sup>&25°C)

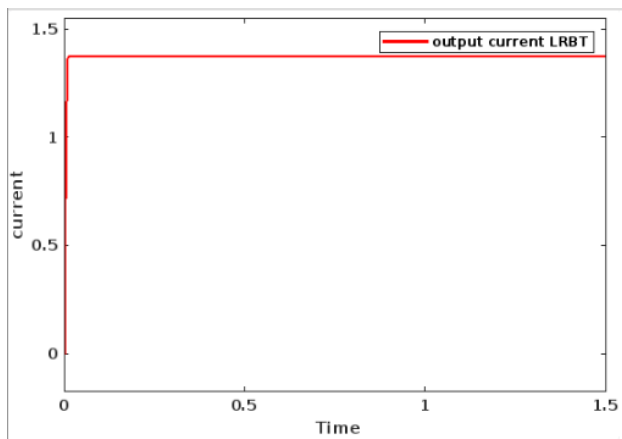


Figure 15. Load output current under PSC2(800Watt/m<sup>2</sup>, 25°C) with LRBT

### 5.1. Efficiency of Controller under varying weather conditions

Equation (17) is used to calculate the power efficiency of both the conventional and proposed controllers to evaluate the effectiveness of the LRBT-MPPT controller.

$$\text{Efficiency} = (\text{Pout}/\text{Pin}) * 100 \tag{17}$$

Where Pout is the average power output of the SEPIC controller under all operating conditions, and Pin is the steady average input power to the controller. Figure 17 illustrates the tracking efficiency under PSC-1, PSC-2, and PSC-3. The LRBT-MPPT controller demonstrates the highest tracking efficiency under varying climatic conditions.

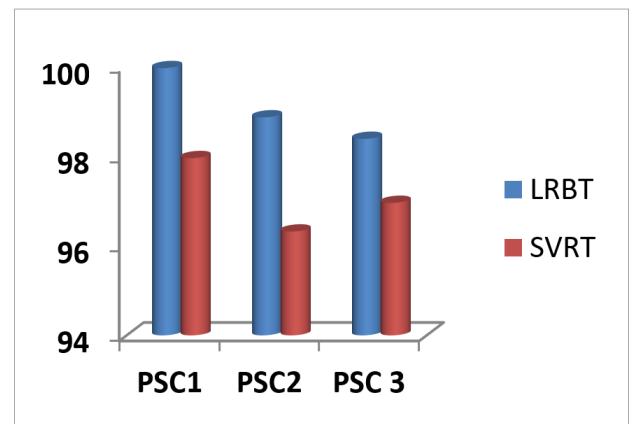


Figure 17. Comparison of tracking efficiency under PSC-1, PSC-2, and PSC-3

### 6. Conclusion

A sophisticated LRBT-MPPT controller was proposed using a SEPIC converter. The performance of this controller was verified through comparison with the SVRT approach. The results indicate that the proposed method is more advantageous due to its features, which include rapid convergence, improved efficiency exceeding 98% in all tested shading scenarios, and minimal variations at the steady state. It significantly reduces oscillations under equilibrium conditions and demonstrates excellent dynamic performance. In this paper, a novel controller built using regression-based machine learning was presented. The key points are as follows:

- I. LRBT achieved a mean efficiency  $\eta = 98.3\% \pm 0.25$ , compared to SVRT.
- II. The proposed system operates in real-time and provides high tracking speed, with a tracking time of 0.10 s (variance 0.0008 s), a low root mean square

error (RMSE) of 0.01689, and minimal steady-state fluctuations.

- III. The LRBT model size is 4 KB, with a prediction speed of approximately 4800 observations per second, making it suitable for deployment on microcontrollers.

**Future Work:** Leveraging the promising results of the LRBT-MPPT controller, subsequent studies may explore several avenues to enhance performance and expand applicability:

- **Hardware Deployment and Real-Time Assessment:** Transitioning from MATLAB simulations to actual hardware implementation with real-world sensors and converters will validate the controller's robustness and performance under practical conditions, including noisy environments and imperfect components.
- **Adaptation to Various Climate Scenarios:** Enhancing the model to flexibly respond to different weather patterns, seasonal changes, and harsh conditions through online learning or adaptive machine learning techniques.
- **Investigation of Hybrid or Ensemble Machine Learning Models:** Combining regression with other machine learning or deep learning approaches to improve tracking accuracy and speed, particularly under rapidly fluctuating irradiance conditions.

## Acknowledgement

The authors would like to express their sincere thankfulness to all those who contributed directly or indirectly to the successful completion of this research work. We are deeply thankful to Meerut Institute of Technology Meerut for providing the necessary facilities, academic environment, and moral support required for this research.

## NOMENCLATURE

PV	Photovoltaic
SPVS	Solar Photovoltaic System
MPPT	Maximum Power Point Tracking
P-VC	Power Voltage Characteristics
MxPP	Maximum Power Point
SEPIC	Single-Ended Primary Inductor Converter
PSC	Partial Shading Condition
GPPP	Global Peak Power Point
LPPPs	Lower Peak Power Point
$V_{in}$	Input voltage (V)
$I_{in}$	Input current (A)
$V_{out}$	Output Voltage
$I_{out}$	Output current
$P_{out}$	Output power (W)
$\eta$	Tracking efficiency (%)
CC	Computational Complexity
T	Tracking Time
OP	Output Power
OC	Output Current
Rsh	Shunt Resistance, Rx: Series Resistance
$I_d$	Diode Current
$I_{sp}$	Incident solar panel current
$I_{px}$	shunt leakage current
$I_p$	Output Current
$I_s$	Saturation Current
nz	array configuration ratio
$N_y$	Series Module
$N_p$	Parallel module

A	Diode ideality factor between 1 or 2
K	Boltzman constant $1.381 \times 10^{-23}$ J/K
T	Cell temperature in K
Pno	Perturb & Observation algorithm
HCg	Hill Climbing algorithm
INCA	Incremental Conductance algorithm
FLC	Fuzzy Logic Control
INC-DFO	Incremental Conductance – Dragonfly Optimization
LRBT	Linear Regression Based Technique
SVRT	Support Vector Regression Technique
ELM	Extreme Learning Algorithm
DTR	Decision Tree Regression
ANN	Artificial Neural Network
BNN	Bayesian Neural Network
MVLR	Multiple variable linear regression algorithm
SVM	Support Vector Machine
DE	Differential Evolution based algorithm

## References

1. Abo-Elyousr, F. K., Abdelshafy, A. M., & Abdelaziz, A. Y. (2019). MPPT-Based particle swarm and cuckoo search algorithms for PV systems. In *Green energy and technology* (pp. 379–400). [https://doi.org/10.1007/978-3-030-05578-3\\_14](https://doi.org/10.1007/978-3-030-05578-3_14)
2. Ahmed, J., & Salam, Z. (2014). A Maximum Power Point Tracking (MPPT) for PV system using Cuckoo Search with partial shading capability. *Applied Energy*, 119, 118–130. <https://doi.org/10.1016/j.apenergy.2013.12.062>
3. Al Garni, H. Z., Sundaram, A., Awasthi, A., Chandel, R., Tajjour, S., & Chandel, S. S. (2024). A Comprehensive Review of Most Competitive Maximum Power Point Tracking Techniques for Enhanced Solar Photovoltaic Power Generation. *Journal of Renewable Energy and Environment*, 11(3), 60–80. doi: 10.30501/jree.2024.408699.1638
4. Alpaydin, E. (n.d.). *Introduction to machine learning*. MIT Press.
5. Awan, K. S., Mahmood, T., Shorfuzzaman, M., Ali, R., & Mehmood, R. M. (2021). A machine learning based algorithm to process partial shading effects in PV arrays. *Computers, Materials & Continua/Computers, Materials & Continua (Print)*, 68(1), 29–43. <https://doi.org/10.32604/cmc.2021.014824>
6. Batarseh, M. G., & Za'fer, M. E. (2018). Hybrid maximum power point tracking techniques: A comparative survey, suggested classification and uninvestigated combinations. *Solar Energy*, 169, 535–555. <https://doi.org/10.1016/j.solener.2018.04.045>
7. Bayrak, F., Oztop, H. F., & Selimefendigil, F. (2019). Effects of different fin parameters on temperature and efficiency for cooling of photovoltaic panels under natural convection. *Solar Energy*, 188, 484–494. <https://doi.org/10.1016/j.solener.2019.06.036>
8. Bayrak, F., Oztop, H. F., & Selimefendigil, F. (2020). Experimental study for the application of different cooling techniques in photovoltaic (PV) panels. *Energy Conversion and Management*, 212, 112789. <https://doi.org/10.1016/j.enconman.2020.112789>
9. Beers, B. (2024, August 1). *Regression: definition, analysis, calculation, and example*. Investopedia. <https://www.investopedia.com/terms/r/regression.asp>
10. Belghith, O. B., Sbitta, L., & Bettaher, F. (2016). MPPT Design Using PSO Technique for Photovoltaic System Control Comparing to Fuzzy Logic and P&O Controllers. *Energy and Power Engineering*, 08(11), 349–366. <https://doi.org/10.4236/epe.2016.811031>
11. Du, Y., Yan, K., Ren, Z., & Xiao, W. (2018). Designing localized MPPT for PV systems using Fuzzy-Weighted Extreme Learning Machine. *Energies*, 11(10), 2615. <https://doi.org/10.3390/en11102615>
12. Farayola, A. M., Sun, Y., & Ali, A. (2018). Optimization of PV systems using Linear Interactions Regression MPPT techniques. *2022 IEEE PES/IAS PowerAfrica*, 545–550. <https://doi.org/10.1109/powerAfrica.2018.8521064>

13. G Tandel, B., & R Vora, D. (2016). MPP detection based on genetic algorithm for PV system in partial shading condition. *International Journal for Research & Development in Technology*, 5(4). <https://www.ijrdt.org/upload/73919IJRDTVLIS54-5418.pdf>
14. Gökkuş, G., & Endiz, M. S. (2024). Modeling and simulation of SEPIC converter based solar simulator circuit for accurate testing and analysis under varying solar radiation conditions. *Journal of Radiation Research and Applied Sciences*, 17(4), 101070. <https://doi.org/10.1016/j.jrras.2024.101070>
15. Gupta, A. K., Chauhan, Y. K., & Maity, T. (2018). Experimental investigations and comparison of various MPPT techniques for photovoltaic system. *Sadhana*, 43(8). <https://doi.org/10.1007/s12046-018-0815>
16. Hayder, W., Oglari, E., Dolara, A., Abid, A., Hamed, M. B., & Sbita, L. (2020). Improved PSO: A Comparative Study in MPPT Algorithm for PV System Control under Partial Shading Conditions. *Energies*, 13(8), 2035. <https://doi.org/10.3390/en13082035>
17. Ishrat, Z., Ali, K. B., Vats, S., & Kumar, S. (2023). Optimizing solar energy harvesting: Supervised Machine Learning-Driven Peak Power Point tracking for diverse weather conditions. *International Journal of Robotics and Control Systems*, 3(4), 1007–1020. <https://doi.org/10.31763/ijrcs.v3i4.1176>
18. Ishrat, Z., Vats, S., Ali, K. B., Shah, O. A., & Ahmed, T. (2023). *A Comprehensive Study on Conventional HPPT Techniques for Solar PV System* (pp. 315–321). <https://doi.org/10.1109/cictn57981.2023.10140264>
19. Ishrat, Z., Gupta, A. K. & Nayak, S. (2024). A Comprehensive Review of MPPT Techniques Based on ML Applicable for Maximum Power in Solar Power Systems, *Journal of Renewable Energy and Environment (JREE)*, 11(1), 28-37. <https://doi.org/10.30501/jree.2023.385661.1556>
20. Ishrat, Z., Kumar Gupta A. & Nayak, S. (2024). Optimizing Photovoltaic Arrays: A Novel Approach to Maximize Power Output in Varied Shading Patterns, *Journal of Renewable Energy and Environment (JREE)*, 11(2), 75-88. <https://doi.org/10.30501/jree.2023.415011.1674>
21. Kalogerakis, C., Koutroulis, E., & Lagoudakis, M. G. (2020). Global MPPT Based on Machine-Learning for PV Arrays Operating under Partial Shading Conditions. *Applied Sciences*, 10(2), 700. <https://doi.org/10.3390/app10020700>
22. Kamarzaman, N. A., & Tan, C. W. (2014). A comprehensive review of maximum power point tracking algorithms for photovoltaic systems. *Renewable and Sustainable Energy Reviews*, 37, 585–598. <https://doi.org/10.1016/j.rser.2014.05.045>
23. Karami, N., Moubayed, N., & Outbib, R. (2016). General review and classification of different MPPT Techniques. *Renewable and Sustainable Energy Reviews*, 68, 1–18. <https://doi.org/10.1016/j.rser.2016.09.132>
24. Keyrouz, F. (2018a). Enhanced Bayesian based MPPT controller for PV systems. *IEEE Power and Energy Technology Systems Journal*, 5(1), 11–17. <https://doi.org/10.1109/jpets.2018.2811708>
25. Khan, M., Khan, M. M., Irfan, M., Ahmad, N., Haq, M. A., Khan, I., & Mousa, M. (2022). Energy performance enhancement of residential buildings in Pakistan by integrating phase change materials in building envelopes. *Energy Reports*, 8, 9290–9307. <https://doi.org/10.1016/j.egyr.2022.07.047>
26. Kumar Panda, S., & Kumar, P. (2023). Machine Learning and its algorithm and development analysis. *International Journal of Advanced Research in Science, Communication and Technology (IJARSCT)*, 3. <https://ijarsct.co.in/A10041.pdf>
27. Liu, Y., Chen, J., & Huang, J. (2014). A review of maximum power point tracking techniques for use in partially shaded conditions. *Renewable and Sustainable Energy Reviews*, 41, 436–453. <https://doi.org/10.1016/j.rser.2014.08.038>
28. Mahesh, P. V., Meyyappan, S., & Alla, R. R. (2022). Maximum power point tracking using decision-tree machine-learning algorithm for photovoltaic systems. *Clean Energy*, 6(5), 762–775. <https://doi.org/10.1093/ce/zkac057>
29. Manickam, C., Raman, G. R., Raman, G. P., Ganesan, S. I., & Nagamani, C. (2016). A Hybrid Algorithm for Tracking of GMPP Based on P&O and PSO With Reduced Power Oscillation in String Inverters. *IEEE Transactions on Industrial Electronics*, 63(10), 6097–6106. <https://doi.org/10.1109/tie.2016.2590382>
30. Martínez, D. D., Codomiu, R. T., Giral, R., & Seisdedos, L. V. (2021). Evaluation of particle swarm optimization techniques applied to maximum power point tracking in photovoltaic systems. *International Journal of Circuit Theory and Applications*, 49(7), 1849–1867. <https://doi.org/10.1002/cta.2978>
31. Memaya, M., Moorthy, C. B., Tahiliani, S., & Sreeni, S. (2019). Machine learning based maximum power point tracking in solar energy conversion systems. *International Journal of Smart Grid and Clean Energy*, 662–669. <https://doi.org/10.12720/sgce.8.6.662-669>
32. Mohapatra, A., Nayak, B., Das, P., & Mohanty, K. B. (2017). A review on MPPT techniques of PV system under partial shading condition. *Renewable and Sustainable Energy Reviews*, 80, 854–867. <https://doi.org/10.1016/j.rser.2017.05.083>
33. Mohri, M., Rostamizadeh, A., & Talwalkar, A. (2018). *Foundations of Machine Learning, second edition*. MIT Press.
34. Moon, A. H., Mehruz, S., & Ahmad, S. (2022). Design and implementation of SEPIC Converter for PV System based Smart Home Application (pp. 1–6). <https://doi.org/10.1109/stpes54845.2022.10006540>
35. Mosa, M., Shadmand, M. B., Balog, R. S., & Rub, H. A. (2017). Efficient maximum power point tracking using model predictive control for photovoltaic systems under dynamic weather condition. *IET Renewable Power Generation*, 11(11), 1401–1409. <https://doi.org/10.1049/iet-rpg.2017.0018>
36. Mustafa, R. J., Goma, M. R., Al-Dhaifallah, M., & Rezk, H. (2020). Environmental impacts on the performance of solar photovoltaic systems. *Sustainability*, 12(2), 608. <https://doi.org/10.3390/su12020608>
37. Nkambule, M. S., Hasan, A. N., Ali, A., Hong, J., & Geem, Z. W. (2020). Comprehensive evaluation of machine learning MPPT algorithms for a PV system under different weather conditions. *Journal of Electrical Engineering and Technology*, 16(1), 411–427. <https://doi.org/10.1007/s42835-020-00598-0>
38. Nugraha, D. A., Lian, K. L., & Suwarno, N. (2019). A novel MPPT method based on Cuckoo search algorithm and Golden Section search algorithm for partially shaded PV system. *Canadian Journal of Electrical and Computer Engineering*, 42(3), 173–182. <https://doi.org/10.1109/cjeece.2019.2914723>
39. Piegari, L., Rizzo, R., Spina, I., & Tricoli, P. (2015). Optimized adaptive perturb and observe maximum power point tracking control for photovoltaic generation. *Energies*, 8(5), 3418–3436. <https://doi.org/10.3390/en8053418>
40. Pilakkat, D., Kanthalakshmi, S., & Navaneethan, S. (2020). A Comprehensive Review of Swarm Optimization Algorithms for MPPT Control of PV Systems under Partially Shaded Conditions. *Electronics ETF*, 24(1). <https://doi.org/10.7251/els2024003p>
41. Podder, A. K., Roy, N. K., & Pota, H. R. (2019). MPPT methods for solar PV systems: a critical review based on tracking nature. *IET Renewable Power Generation*, 13(10), 1615–1632. <https://doi.org/10.1049/iet-rpg.2018.5946>
42. Priyadarshi, N., Padmanaban, S., Holm-Nielsen, J. B., Blaabjerg, F., & Bhaskar, M. S. (2019). An experimental estimation of hybrid ANFIS–PSO-Based MPPT for PV grid integration under fluctuating sun irradiance. *IEEE Systems Journal*, 14(1), 1218–1229. <https://doi.org/10.1109/jsyst.2019.2949083>
43. Putri, B. R., Sudiharto, I., Ferdiansyah, I., Karso, A. B., & Yanaratri, D. S. (2021). Design SEPIC converter for battery charging using solar panel. *Journal of Physics Conference Series*, 1844(1), 012015. <https://doi.org/10.1088/1742-6596/1844/1/012015>
44. Radjai, T., Rahmani, L., Mekhilef, S., & Gaubert, J. P. (2014). Implementation of a modified incremental conductance MPPT algorithm with direct control based on a fuzzy duty cycle change estimator using dSPACE. *Solar Energy*, 110, 325–337. <https://doi.org/10.1016/j.solener.2014.09.014>
45. Ram, J. P., Babu, T. S., & Rajasekar, N. (2016). A comprehensive review on solar PV maximum power point tracking techniques. *Renewable and Sustainable Energy Reviews*, 67, 826–847. <https://doi.org/10.1016/j.rser.2016.09.076>

46. Rasmussen, C. E. (2004). Gaussian processes in machine learning. In *Lecture notes in computer science* (pp. 63–71). [https://doi.org/10.1007/978-3-540-28650-9\\_4](https://doi.org/10.1007/978-3-540-28650-9_4)
47. Rawat, A. S., & Chandel, S. S. (2013). Hill Climbing Techniques for Tracking Maximum Power Point in Solar Photovoltaic Systems: A Review. *International Journal of Sustainable Development and Green Economics*, 2(1), 90–95.
48. Rezk, H., Fathy, A., & Abdelaziz, A. Y. (2017a). A comparison of different global MPPT techniques based on meta-heuristic algorithms for photovoltaic system subjected to partial shading conditions. *Renewable and Sustainable Energy Reviews*, 74, 377–386. <https://doi.org/10.1016/j.rser.2017.02.051>
49. Sarwar, S., Javed, M. Y., Jaffery, M. H., Arshad, J., Rehman, A. U., Shafiq, M., & Choi, J. (2022). A Novel Hybrid MPPT Technique to Maximize Power Harvesting from PV System under Partial and Complex Partial Shading. *Applied Sciences*, 12(2), 587. <https://doi.org/10.3390/app12020587>
50. Sattar, M., Rehman, A., Ahmad, N., Mohammad, A., Ahmadi, A. a. A., & Ullah, N. (2022). Performance analysis and optimization of a cooling system for hybrid solar panels based on climatic conditions of Islamabad, Pakistan. *Energies*, 15(17), 6278. <https://doi.org/10.3390/en15176278>
51. Sharmin, R., Chowdhury, S. S., Abedin, F., & Rahman, K. M. (2022). Implementation of an MPPT technique of a solar module with supervised machine learning. *Frontiers in Energy Research*, 10. <https://doi.org/10.3389/fenrg.2022.932653>
52. Sun, S., Cao, Z., Zhu, H., & Zhao, J. (2019). A survey of optimization methods from a machine learning perspective. *IEEE Transactions on Cybernetics*, 50(8), 3668–3681. <https://doi.org/10.1109/tycb.2019.2950779>
53. Takruri, M., Farhat, M., Barambones, O., Ramos-Hernanz, J. A., Turkieh, M. J., Badawi, M., AlZoubi, H., & Sakur, M. A. (2020). Maximum power point tracking of PV system based on machine learning. *Energies*, 13(3), 692. <https://doi.org/10.3390/en13030692>
54. Takun, P., Kaitwanidvilai, S., & Jettanasen, C. (2011). *Maximum power point tracking using fuzzy logic control for photovoltaic systems*. [http://www.iaeng.org/publication/IMECS2011/IMECS2011\\_pp986-990.pdf?origin=publication\\_detail](http://www.iaeng.org/publication/IMECS2011/IMECS2011_pp986-990.pdf?origin=publication_detail)
55. Tey, K. S., Mekhilef, S., Seyedmahmoudian, M., Horan, B., Oo, A. T., & Stojcevski, A. (2018). Improved differential Evolution-Based MPPT algorithm using SEPIC for PV systems under partial shading conditions and load variation. *IEEE Transactions on Industrial Informatics*, 14(10), 4322–4333. <https://doi.org/10.1109/tii.2018.2793210>